



DOI: 10.18720/MCE.93.4

Long span bridges buffeting response to wind turbulence

R.N. Guzeev^a, A. Domaingo^b

^a St. Petersburg State University of Architecture and Civil Engineering, St. Petersburg, Russia

^b ALLPLAN Infrastructure GmbH, Graz, Austria

* E-mail: guzeev.roman@gmail.com

Keywords: cable stayed and suspension bridges, buffeting response, turbulence model, bridge deck, structural design, coherence, random vibration, numerical models.

Abstract. The buffeting response of the cable-supported bridges is studied. Several wind turbulence models are summarized and wind field models for practical application in bridge and structural engineering is proposed. The wind turbulence model comprises the mean wind and turbulence intensity profile, power spectral density and coherence functions. The dynamic response of the structure is governed by random vibration theory of stationary random process. The simplified method of analysis using the mode decomposition method is proposed where the only main modes are considered and the aerodynamic damping is introduced by means of flutter derivatives. The method of cable system coherence analysis is presented. The calculation procedure of generalized power spectral densities of wind turbulence load for different structural component is proposed. This procedure takes into account the effects of all three orthogonal components of wind turbulence. The contribution of the wind velocity components into total dynamic response and their correlation for different structural elements is studied.

1. Introduction

Slender cable-stayed structures, especially bridges are vulnerable to wind action and prone to significant dynamic response to natural wind turbulence. Wind turbulence near the ground is produced by the boundary layer of wind flow at the height 300-400 m [1, 2]. This is a layer where the structure has to be built.

The cable-stayed or suspension bridge has three main structural components such as the bridge deck girder, pylons and cables. All of them have different interaction with the wind flow. At every structural element six component forces are acting which consist of three steady state forces and three moments.

The bridge deck can be considered as a prismatic 2D body with specific cross-section. For example, the cross-section can be a monobox girder (Golden Horn Bay Bridge, Russky Island Bridge, Russia) or a double deck girder (Stonecutters Bridge, China and bridge over Peter The Grate Channel, Russia). Steady state aerodynamic forces can be reduced to drag D and lift L forces and torsion (pitch) moment M (Figure 1). Torsional and vertical frequency of the cable-stayed bridge deck are well separated. Usually torsional frequency is 1.5–3.0 times higher than vertical one.

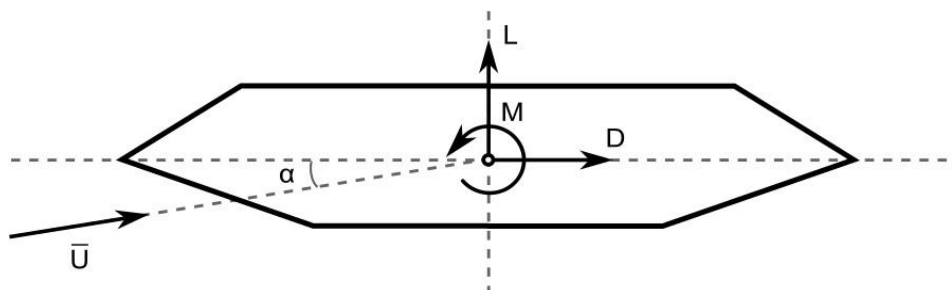


Figure 1. Aerodynamic forces.

Guzeev, R.N., Domaingo, A. Long span bridges buffeting response to wind turbulence. Magazine of Civil Engineering. 2020. 93(1). Pp. 35–49. DOI: 10.18720/MCE.93.4

Гузев Р.Н., Доминго А. Реакция большепролетных мостов на турбулентный ветровой поток // Инженерно-строительный журнал. 2020. № 1(93). С. 35–49. DOI: 10.18720/MCE.93.4



This work is licensed under a CC BY-NC 4.0

Aerodynamic forces acting on the pylon can be described by only drag and lift forces. The torsional moment can be neglected due to the relatively high torsional stiffness. For symmetric cross sections, the lift forces do not produce significant effect on wind response. For non-symmetrical cross-sections, the lift force must be considered as well as the drag force. Besides, first derivatives of aerodynamic coefficients by the angle of incidence significantly influence the static and dynamic stability of the structure, e.g. torsional divergence and across wind galloping, respectively [3].

In order to linearize the problem fluctuation components are considered as small values and only linear terms remain in the expression for wind pressure, effective angle of incidence and wind load coefficients expansion. In the most general case, also the relative velocity due to the moving structure must be considered. In the present study the effect of moving structure is considered only in terms of aerodynamic damping and evaluated by the means of the flutter derivatives.

The conventional approach to the turbulence wind action such as that in chimneys, truss towers, masts and simple buildings considers only along wind component of the wind fluctuation velocity [4, 5]. Turbulence action on cable-stayed bridges requires consideration of all three components. The vertical component for the bridge deck and the transversal component for pylons produce changes in the mean wind angle of incidence. This subsequently causes dynamic response because the aerodynamic coefficients, particularly lift coefficient, strongly depend on the angle of incidence [6, 7].

For cables with circular symmetrical cross-section it is enough to take into account only the drag force.

Steady-state forces can be described by the means of steady-state aerodynamic coefficients which can be obtained through wind tunnel tests or CFD analysis [6, 7]. The most reliable aerodynamic properties are given by wind tunnel cross section tests at the fine scale. CFD analysis also gives good results but requires highly professional approach and adjustment of the wind flow model to the specific purpose.

Wind velocity comprises the mean wind velocity vector and three orthogonal fluctuation components.

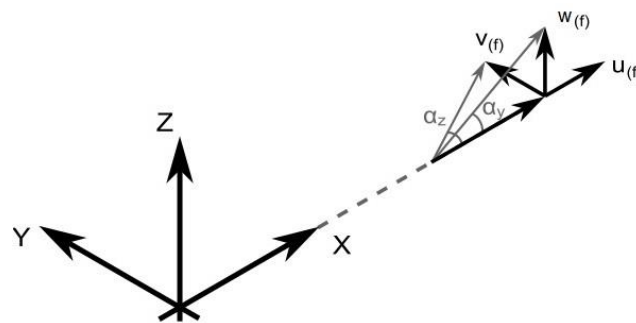


Figure 2. Orthogonal fluctuation components of wind flow.

Pylons with two or more legs with transversal wind direction produce a shadow effect for the downwind leg. Reduction in the wind force for the downwind leg can be taken into account by introducing the shadow coefficient. The value of such coefficient as estimated by CFD analyses and wind tunnel tests for common pylon structures with A-shaped pylons is about 0.6–0.7.

The wind turbulence fluctuation velocity is considered to be a stationary ergodic random process. The full model of the wind field sufficient to calculate the structural response should include the mean wind velocity profile, turbulence intensity profile, power spectral density and root coherence function. This metrological data should be derived through long-term monitoring in several points on site [8, 9] or numerical modeling [10]. However, it is acceptable to use generalized models such as [1, 2, 4, 5].

The buffeting analysis basics for line-like slender structures was established by Davenport 1960's [11]. The proposed method is employed idea that variance of response can be represented by background and resonance response. The authors [12] modified Davenport's method and took into account only the deck of the bridge and coherence along the bridge axis for cable stayed bridge with main span 400 m where effect of cables is moderate. The cable-stayed bridges buffeting response taking into account heave, pitch and torsional modes was studied in [7]. The buffeting response of the extremely long Stonecutters cable-stayed bridge is studied in [13, 14], taking into account the deck aerodynamic properties and coherence along the bridge.

Experimental and analytical studies of buffeting response and wind field at bridge sites are given in [8, 9, 15–17]. The authors [5, 18] and national codes [1, 2, 4] proposed different approach for analytical description of wind turbulent flow.

For the extremely long cable-stayed bridges, the cables assume a significant amount of the wind load because the cables system for such bridges form a sort of 3D "sails" and spatial coherence shall be analyzed. The wind load affect both the pylons and the deck. Consideration all components of wind turbulence is crucial for long span cable-stayed bridges buffeting analysis.

This paper is devoted to comprehensive study of buffeting response for long span cable-stayed bridges and comprises turbulence model for practical application, analytical description of aerodynamic interaction between wind flow and structural elements, consideration of three components of wind turbulence and spatial coherence for cable system, deck and pylons.

This paper is dedicated to the analysis of dynamic response to the wind natural turbulence. Other aeroelastic phenomena is out of scope. The flutter critical wind velocity for the bridge structure must be much higher than the design wind velocity. In contrary, vortex shedding lock-in vibration usually occurs for the relatively low wind velocity where the effect of wind turbulence could be neglected. The negative aerodynamic damping is not allowed for the bridge structures within design wind speed. Thus, galloping and other aerodynamic instability caused by negative damping is not considered in the article.

2. Methods

2.1. Wind turbulence model

The mean wind profile is described by logarithmic or power law. Both profiles depend on the type of the surrounding terrain. The logarithmic law uses the parameter of terrain roughness. The power law takes into account the terrain effect by introducing different exponents. We can obtain the mean wind velocity by multiplying the wind profile coefficient by the base wind velocity at the height of 10 m. The base wind velocity is available, for example, in [5, 18] or using local measurement.

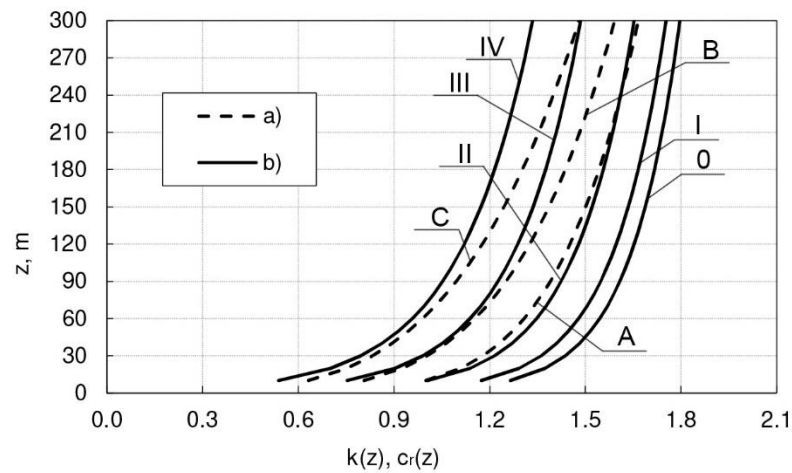


Figure 3. Mean wind velocity coefficient profile:
a) the power law for terrain A, B, C [8]; b) the logarithmic law for terrain 0-IV [6].

To be on the safe side, the logarithmic law is more preferable for structures located on the regular terrain covered with vegetation and buildings. Meanwhile, for the open terrain both profiles are very close (Figure 2). This kind of terrain such as rivers, lakes and sea shore correspond to the typical location of a bridge site. However, for bridges in the city surrounded by buildings or high hills the local terrain must be considered [15–17]. Therefore, the logarithmic expression for the mean velocity profile is employed in the present study.

$$c_r = k_r \ln(z / z_0), \quad (1)$$

where z is elevation above ground or water surface;

z_0 is the roughness length;

k_r is the terrain factor.

The values for z_0 and k_r refer to [6].

The most important parameter of wind turbulence is the normalized non-dimension power spectral density of wind fluctuation velocity. The European standard on wind action uses the Kaimal spectrum of along wind component [6]. The American standard slightly modifies the Kaimal spectrum. This spectrum has limitation of application with height 200 m. Russian, Chinese and Canadian codes use the Davenport spectrum for this component [5]. The Davenport spectrum has significant disadvantages because it does not depend on the height and turbulence length scale is constant. However, applying the Davenport spectrum is much easier for dynamic structural analysis. In this case, for simple structures with the simple mode shape, calculation can be made by hand. The Karman spectrum is also widely used in structural analysis and national wind engineering standards. The Australian and Japanese documents have adopted the Karman spectrum. The Karman spectrum with modification in high frequency range is given in Engineering Science Data Unit (ESDU) [1, 2]. Besides, the new

Karman spectra are given there for the full range of frequencies. However, for cable-stayed structures with relatively low natural frequencies the Karman spectrum Equation (2) can be used.

$$\frac{fS_{uu}(f)}{\sigma_u^2} = \frac{4n_u}{(1+70.8n_u^2)^{5/6}}, \quad (2)$$

where $S_{uu}(f)$ is the PSD function of along wind component;

σ_u is the standard deviation of along wind component;

f is the frequency in Hz;

n_u is the non-dimensional frequency.

The non-dimensional form of spectral density requires non-dimensional frequency normalized by the wind velocity and integral turbulence length scale $n_u = fL_u / \bar{U}(z)$. The integral turbulence length scale represents the average size of turbulence eddies.

The sophisticated expression for the modified and Karman spectra and the turbulence length scale is given in [1, 2].

For practical application the power Counihan turbulence length scale can be employed [19].

$$L_u = 300(z/300)^{0.46+0.074\ln(z_0)}. \quad (3)$$

The Davenport spectrum for along wind component uses the constant integral length scale and it is equal to 1200 m.

From many field measurements [20], the turbulence length scale for along wind component corresponds to the length scale for vertical and transversal components in the following ratio:

$$L_v \approx L_u / 3; \quad L_w \approx L_u / 9. \quad (4)$$

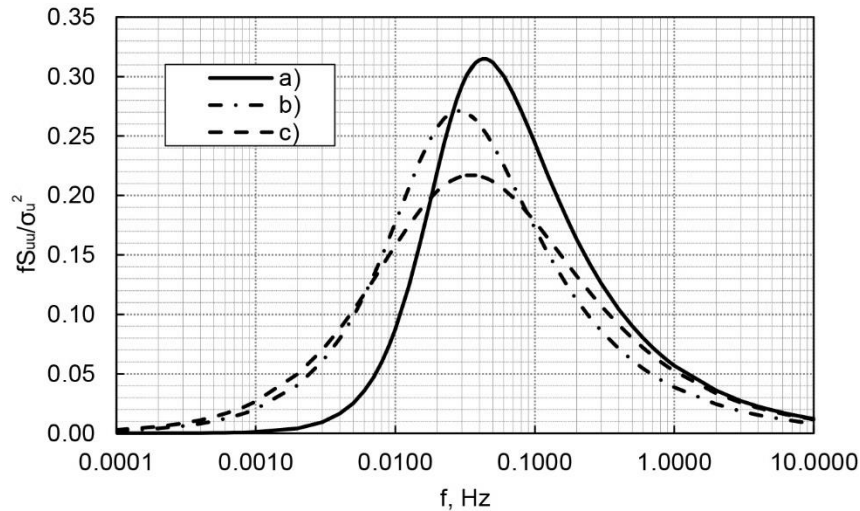


Figure 4. Normalized PSD spectrum of longitudinal component:
a) the Davenport spectra, b) the Karman spectra, c) the Kaimal spectrum.

The vertical and transversal components as it was mentioned above, are important as well as the along wind component. For these components there exists the various representation of the spectrum. For practical application the Karman spectra [1] give a good approximation in the absence of field measurements and monitoring.

$$\frac{fS_{ii}(f)}{\sigma_i^2} = \frac{4n_i(1+755.2n_i^2)}{(1+283.2n_i^2)^{11/6}}, \quad (5)$$

where $I = v, w$ is the notation of the turbulence components direction;

$S_{ii}(f)$ is the PSD function for vertical and transversal components;

n_i is the non-dimensional frequency.

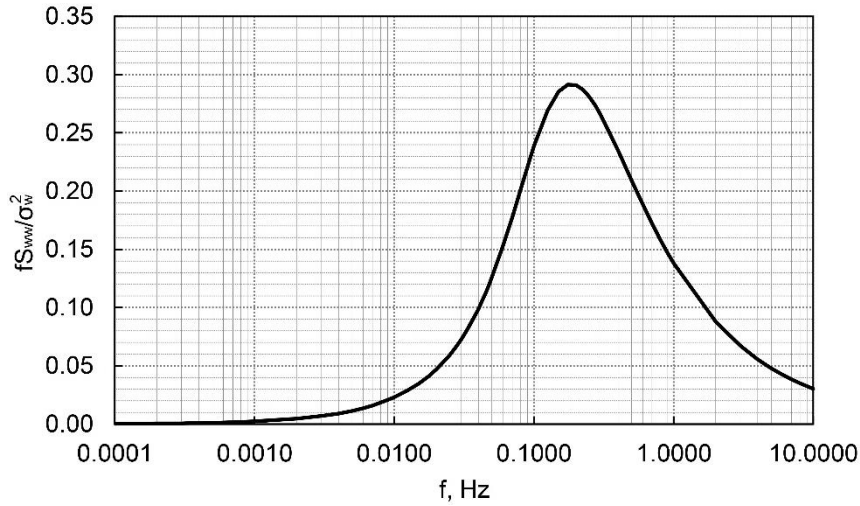


Figure 5. Normalized PSD spectrum of vertical component.

We have to complete the description of wind velocity component power spectral densities with the cross spectra of along wind and vertical components and the vertical and transversal component. Actually, this component has complex value. For simplified analysis, the cross spectra can be neglected in the assumption of the statistically independent along wind and vertical component as well as the transversal component but this assumption seems to be incorrect because the structure is located in the anisotropic turbulence boundary layer. The imaginary part can be neglected because it contributes nothing to the maximal structural response. Because of the turbulence eddies moving pattern, the real part of the cross spectrum has to be negative. In this study we employ the following expression for the cross spectrum [12].

$$\frac{fS_{uv}(f)}{u_*^2} = -\frac{14fz/\bar{U}(z)}{(1+9.6fz/\bar{U}(z))^{2.4}} \tag{6}$$

The standard deviation of wind fluctuation velocity is described by the turbulence intensity profile. Turbulence intensity is the ratio of the standard deviation to the mean wind velocity. Sophisticated expressions of the turbulence intensity based on the field measurement refer to [1]. The formulation of the turbulence intensity is closely related to the power spectral density shape. Eurocode [4] uses the logarithmic expression, meanwhile the Davenport spectrum uses the power law for turbulence intensity [5]. In the present study for the purposes of structural analysis of cable supported structures we use the logarithmic law.

$$I_u(z) = \frac{\sigma_u}{\bar{U}(z)} = \frac{1}{\ln(z/z_0)} \tag{7}$$

For relatively small terrain roughness, the power law and logarithmic law are barely different. However, for significant roughness, the difference in turbulence intensity profiles is significant and the logarithmic law is more conservative in terms of structural response.

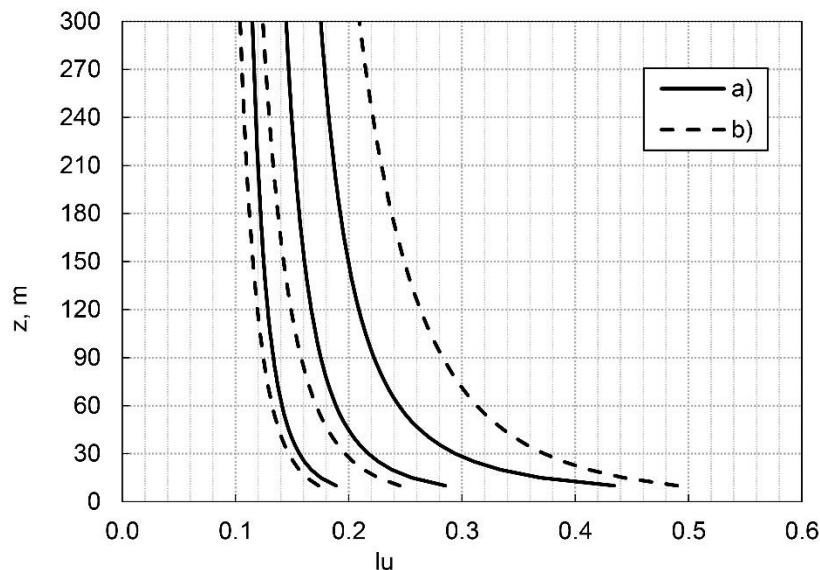


Figure 6. Turbulence intensity profile: a) logarithmic low [7]; b) power low [8].

Based on the observations the known relation between turbulence intensity components is employed in this study [20]:

$$I_v = 0.5I_u; \quad I_w = 0.75I_u. \quad (8)$$

For continuous structures such as the bridge deck, it is important to take into account the correlation of the turbulence eddies between two points i and j in the space. This is done by means of the root coherence function $\chi(\omega)$ [21].

$$S(\omega)_{ij} = \sqrt{S(\omega)_{ii}S(\omega)_{jj}} \chi(\omega). \quad (9)$$

It is a common approach to use the exponential decay function (Equation (10)).

$$\chi_{ii}(\omega)_{ij} = \exp\left(-\frac{\omega \sqrt{C_{l,x}^2(x_i - x_j)^2 + C_{l,y}^2(y_i - y_j)^2 + C_{l,z}^2(z_i - z_j)^2}}{\pi(\bar{U}_i + \bar{U}_j)}\right). \quad (10)$$

This idea was first proposed by Davenport. Later, numerous approaches were suggested to estimate the decay coefficients C_l . The present study uses values proposed in [20] and given in the Table 1. The study [5] uses the similar coefficients but instead of the average of mean wind velocity for two points they use the mean wind velocity at the height 10 m. This approach significantly simplifies the structural analysis. Such assumption seems to be artificial from the theoretical point of view and coherence should depend on the value of mean velocity at the points in question. In the present study is employed the general relation for two points (Equation (10)).

Table 1. Root coherence function decay coefficients

Component	x	y	z
u	3.0	10.0	10.0
v	3.0	6.5	6.5
w	0.5	6.5	3.0

For the cross spectrum we introduce the following coherence function in the form proposed in [22].

$$\chi_{uw} = \sqrt{|\chi_{uu}| |\chi_{ww}|}. \quad (11)$$

2.2. Turbulence wind load in the frequency domain

The general wind distributed load on a structural element is calculated using the steady state wind load coefficients, which is expressed as

$$\begin{Bmatrix} D \\ L \\ M \end{Bmatrix} = 1/2\rho B U(t)^2 \begin{Bmatrix} C_D(\alpha(t)) \\ C_L(\alpha(t)) \\ BC_M(\alpha(t)) \end{Bmatrix} \approx 1/2\rho B (\bar{U} + 2\bar{U}u(t) + u(t)^2) \begin{Bmatrix} C_D(\bar{\alpha}) + \frac{\partial C_D}{\partial \alpha} \alpha \\ C_L(\bar{\alpha}) + \frac{\partial C_L}{\partial \alpha} \alpha \\ BC_L(\bar{\alpha}) + B \frac{\partial C_L}{\partial \alpha} \alpha \end{Bmatrix} \quad (12)$$

D, L, M are the drag, lift and pitch moment forces corresponding to the aerodynamic steady state aerodynamic coefficients C_D, C_L, C_M ;

$\rho = 1.225 \text{ kg/m}^3$ is the air density at the average temperature and pressure;

\bar{U} is the mean wind velocity at the element height;

$u(t)$ is along wind turbulence component;

$\alpha(t)$ is the angle of incidence or angle of attack;

$\frac{\partial C_D}{\partial \alpha}, \frac{\partial C_L}{\partial \alpha}, \frac{\partial C_M}{\partial \alpha}$ are first derivatives of the steady state coefficients by angle of incidence.

It should be pointed out, that expression (12) neglects any response of the structure and the vertical fluctuating wind component is not considered for instantaneous wind velocity.

The angle of attack for the turbulence air flow is not constant and depends on the fluctuation velocity. Thus, it can be expressed in the following way:

The tangent of incidence angle can be obtained using a simple geometrical relation:

$$\tan(\alpha_y) = \frac{w(t)}{\bar{U} + u(t)}; \quad \tan(\alpha_z) = \frac{v(t)}{\bar{U} + u(t)}.$$

The assumption about the smallness of pulsation components allows us to change the tangent of angle incidence by its value and expression for angles of incidence can be written down as:

$$\alpha_y = \frac{w(t)}{\bar{U}}; \quad \alpha_z = \frac{v(t)}{\bar{U}}.$$

The wind load for every structural element now takes the following form

$$\begin{Bmatrix} D \\ L \\ M \end{Bmatrix} = \bar{F}_{ae} + \rho \bar{U} B \begin{bmatrix} C_D & \frac{1}{2} \partial C_D / \partial \alpha \\ C_L & \frac{1}{2} \partial C_L / \partial \alpha \\ BC_M & \frac{1}{2} B \partial C_M / \partial \alpha \end{bmatrix} C_{ae} \begin{Bmatrix} u(t) \\ v(t) \\ w(t) \end{Bmatrix}, \quad (13)$$

where \bar{F}_{ae} is the static wind response to mean wind velocity;

C_{ae} is the matrix that convert the turbulence components from the main coordinate system into the local coordinate system of the structural element where steady state coefficients have been determined.

Thus, transfer matrix function between wind turbulence components can be written in the following form

$$H_b(i\omega) = \rho \bar{U} B \begin{bmatrix} C_D & \frac{1}{2} \partial C_D / \partial \alpha \\ C_L & \frac{1}{2} \partial C_L / \partial \alpha \\ BC_M & \frac{1}{2} B \partial C_M / \partial \alpha \end{bmatrix} C_{ae}. \quad (14)$$

It is known from the analytical solution for a thin plate in potential flow that the response to fluctuation velocity is frequency dependent. Therefore for the stream lined deck we have to introduce frequency dependent admittance functions. For thin and streamlined decks, the theoretical Sears $Q_w(k)$ [23] and Horlock $Q_u(k)$ [24] functions can be used that are defined through the Theodorsen function and depends on reduced frequency $k = B\omega / 2\bar{U}$. These functions have complex value and they are shown on the complex plane (Figure 6). For the vertical component, introducing $Q_w(k)$ is justified but for along wind component, it is not. To be on the safe side, in the present study $Q_u(k)$ is neglected and the final transfer matrix is given in the form:

$$H_b(i\omega) = \rho \bar{U} B \begin{bmatrix} C_D & \frac{1}{2} \partial C_D / \partial \alpha \\ C_L Q_w(k) & \frac{1}{2} \partial C_L / \partial \alpha Q_w(k) \\ BC_M Q_w(k) & \frac{1}{2} B \partial C_M / \partial \alpha Q_w(k) \end{bmatrix} C_{ae}. \quad (15)$$

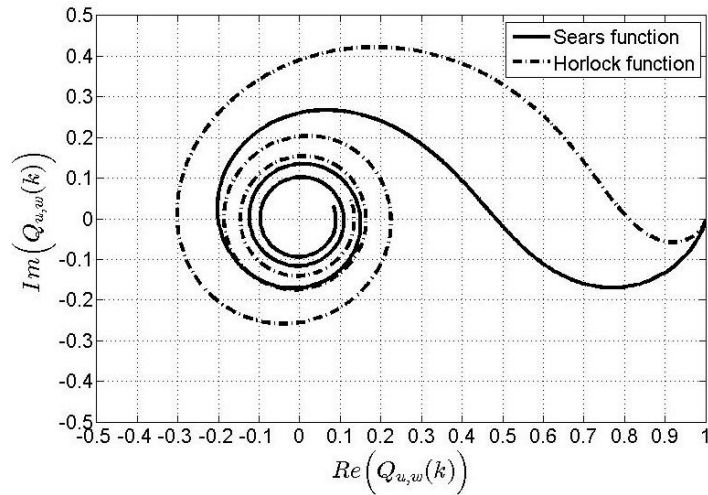


Figure 7. Sears and Horlock function of reduced frequency on complex plain.

Finally, the spectral density of aeroelastic forces for points i and j , the owing relations of stationary random process theory can be written down as following:

$$S_i(\omega)_{ij} = H_b(i\omega) \begin{bmatrix} \chi_{uu}(\omega)S_{uu}(\omega) & \chi_{uv}(\omega)S_{uv}(\omega) & \chi_{uw}(\omega)S_{uw}(\omega) \\ \chi_{uv}(\omega)S_{uv}(\omega) & \chi_{vv}(\omega)S_{vv}(\omega) & 0 \\ \chi_{uw}(\omega)S_{uw}(\omega) & 0 & \chi(\omega)S_{ww}(\omega) \end{bmatrix} \left(H_b(i\omega)^* \right)^T \quad (16)$$

Here the symbol * marks complex conjugate value.

It is known from wind tunnel tests and CFD analysis that aerodynamic admittance functions for the real bridge deck are quite different from the airfoil admittance function [25, 26]. The admittance function usually reduces the dynamic response of the bridge in turbulent flow [25].

At the next step we have to perform the structural analysis in the frequency domain and find the standard deviation and peak response in terms of displacement, acceleration and velocity.

3. Results and Discussion

In the present study the following approach is used for dynamic response analysis. The mean wind velocity and PSD functions for the pylon are defined at the 0.7 H of the pylon height. The wind turbulence parameter for the deck is assumed to be constant and is defined at the deck level.

We are employing natural mode decomposition method and consider only the first lateral, vertical and pitch modes (Figure 6). All these modes we assume to be statistically independent and we neglect correlation between the modal responses. This assumption is valid if the natural frequencies are separated widely enough from each other.

Therefore for each mode the power density of the generalized turbulence load is written down assuming that there is no coupling between deck cables and pylons

$$\begin{aligned} S_{q,x}(\omega) &= S_{x,u}^d(\omega) + S_{x,w}^d(\omega) + S_{x,uw}^d(\omega) + S_{x,u}^p(\omega) + S_{x,u}^c(\omega); \\ S_{q,z}(\omega) &= S_{z,u}^d(\omega) + S_{z,w}^d(\omega) + S_{z,uw}^d(\omega); \\ S_{q,\varphi}(\omega) &= S_{\varphi,u}^d(\omega) + S_{\varphi,w}^d(\omega) + S_{\varphi,uw}^d(\omega), \end{aligned} \quad (17)$$

where $S_{x,u}^d(\omega) = S_u(\omega)(\rho\bar{U}B)^2 C_j^2 \int_0^L \varphi(x') \int_0^L \exp\left(-\frac{C_{uy}f|x-x'|}{\bar{U}}\right) \varphi(x) dx dx'$ is the spectrum caused by the action of longitudinal component at bridge deck and j corresponds to the drag, lift forces and pitch moment;

$S_{x,w}^d(\omega) = S_w(\omega) \left(\frac{1}{2} \rho\bar{U}B\right)^2 \left(\frac{\partial C_j}{\partial \alpha}\right)^2 \int_0^L \varphi(x') \int_0^L \exp\left(-\frac{C_{wy}f|x-x'|}{\bar{U}}\right) \varphi(x) dx dx'$ is spectra caused by the action of the vertical component at bridge deck;

$S_{x,u}^d(\omega) = S_{uw}(\omega)(\rho\bar{U}B)C_j \frac{\partial C_j}{\partial \alpha} \int_0^L \varphi(x') \int_0^L \exp\left(-\frac{C_{wy}f|x-x'|}{\bar{U}}\right) \varphi(x) dx dx'$ is spectra caused by cross power spectral density of the longitudinal and vertical components.

We can obtain in the same manner PSD $S_{x,u}^p(\omega)$ of the wind load on the pylon with integration over the pylon height.

More complicated procedure to calculate participation of cable-stays is presented. The cable-stays have different outer diameter and length. Besides, they are separated in three directions and more precise evaluation of coherence is required.

The modal wind spectral load on the cable system can be evaluated using general approach. The expression for the modal spectrum $S_{x,u}^c$ in the general case,

$$S_{x,u}^c = C_D^2 \iint_G S_u(r, r', \omega) D(r) D(r') \varphi(r) \varphi(r') ds ds', \quad (18)$$

where G is the set of line segments that represent cables system;

$D(r)$ is the cable duct outer diameter;

$\varphi(r)$ is the mode shape along cables system;

The integral in the Equation (18) can be replaced by the sum of integrals over every single cable

$$\begin{aligned} S_{x,u}^c &= C_D^2 \int_G \left(\int_{l_1} S_{uu}(r, r', \omega) D(r) D(r') \varphi(r) \varphi(r') ds + \dots + \int_{l_n} S_{uu}(r, r', \omega) D(r) D(r') \varphi(r) \varphi(r') ds \right) ds' = \\ &= C_D^2 \sum_{\alpha=1}^n \sum_{\beta=1}^n \int_{l_\alpha} \int_{l_\beta} D_\alpha \varphi(r) S_{uu}(r, r', \omega) D_\beta \varphi(r') ds ds'. \end{aligned} \quad (19)$$

In this approach the mode shape is considered constant over cable length and determine in the cable mid node. The cable duct diameter is constant for every single cable. Now we use cross spectrum between points $r(x, y, z)$ and $r'(x', y', z')$ in the form of Equation (9) and (10). Therefore the Equation (19) can be written in matrix form

$$S_{x,u}^c = C_D^2 S_{uu}^c(\omega) \Phi^T J \Phi, \quad (20)$$

where $S_{uu}^c(\omega)$ is PSD spectrum of the longitudinal wind component determined at the average cable height;

Φ is vector of product mode shape φ at cable mid node and their duct diameter;

J is the coherence matrix between cables.

Every element of matrix J can be determined using numerical integration over the cable length as it was done for the bridge deck as following

$$J_{ij} = \int_0^{l_i} \int_0^{l_j} \exp\left(-f \sqrt{C_{xu}(x-x')^2 + C_{yu}(y-y')^2 + C_{zu}(z-z')^2} / \bar{U}\right) ds ds'. \quad (21)$$

Finally, the spectra of modal response and corresponding standard deviation can be now determined using transfer functions

$$S_i(\omega) = |F(i\omega)|^2 S_{q,i}(\omega); \quad (22)$$

$$\sigma_i^2 = \int_0^\infty |F(i\omega)|^2 S_{q,i}(\omega) d\omega = \int_0^\infty \frac{1}{|M(-\omega^2 + 2i\xi_i\omega_i\omega + \omega_i^2)|^2} S_{q,i}(\omega) d\omega, \quad (23)$$

where $i = x, z, \varphi$ is the index of response direction;

ω_i, ξ_i – are the natural cyclic frequency and damping ratio of lateral, vertical and torsional modes;

M is the generalized modal mass.

Let us consider a cable stayed bridge with the main span 1100 m. The results of eigenvalue analysis and the natural frequency are shown on the Figure 8 and Table 2.

Table 2. Natural frequency for basic mode shapes.

Mode shape	Frequency, Hz
Lateral	0.076
Vertical	0.174
Torsional	0.479

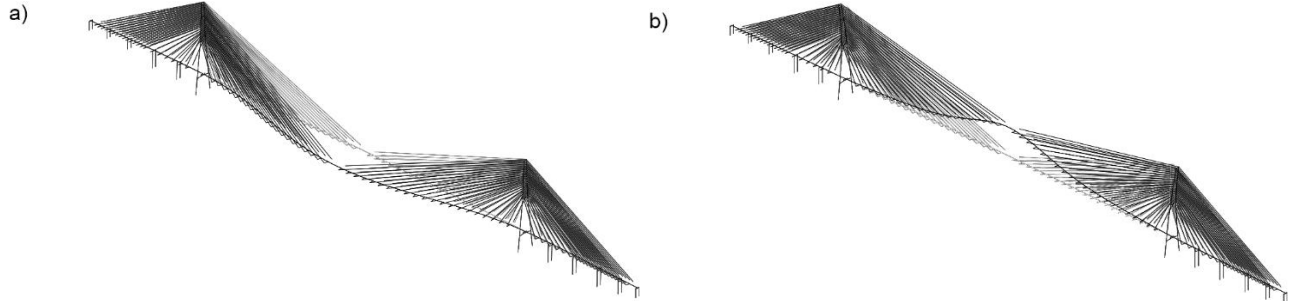


Figure 8. Lateral (a) and vertical (b) mode shapes.

The height of the bridge above water level is 70 m. The design wind mean velocity at the height 10 m is 38 m/s. The roughness of the terrain is $z_0 = 0.01$. The mean wind velocity and turbulence intensity profile are obtained according equation (1) and (7). The PSD function for the wind velocity fluctuation components is described by the expressions (2), (5) and (6).

The steady state coefficients are obtained through the wind tunnel test $C_D = 0.069$; $\partial C_D / \partial \alpha = -0.154$; $C_L = 0.13$ $\partial C_L / \partial \alpha = 3.05$; $C_M = 0.046$; $\partial C_M / \partial \alpha = 0.89$.

The drag coefficient for the pylon is taken equal to 1.70 for upwind leg and 1.02 for downwind leg for mean pylon width of 9 m.

The drag coefficient 0.6 for cables in strong wind is provided by the cable manufacturer.

The damping ratio takes into account structural and aerodynamic damping. The aerodynamic damping for lateral response uses steady state approximation, while for vertical and torsional modes the damping ratio is evaluated by means of flutter derivatives [5], obtained in the cross section wind tunnel test.

$$\begin{aligned}\xi_x &= \xi_s + \frac{2C_D \rho U B}{2\omega_x m}; \\ \xi_z &= \xi_s - \frac{\rho B^2}{2H_1^* m}; \\ \xi_\varphi &= \xi_s - \frac{\rho B^4}{2A_2^* I_p},\end{aligned}\tag{24}$$

where m and I_p are the mass and mass moment of inertia per unit length of the deck;

All three values of the damping ratio is mode dependent and have different value.

$H_1^* = -3.276$, $A_2^* = -0.062$ are flutter derivatives for the vertical and torsional bridge deck displacements obtained for the natural frequencies;

$\xi_s = 0.05$ is the structural damping ratio.

The deck and cables have almost equal drag resistance to mean wind flow and added mass from cables much less then deck mass. For that reason we introduce additional factor 2.0 for ξ_x in Equation (24).

Figure 9 shows the graphs of standard deviation response versus mean wind velocity at the height of 10 m.

We can see that the vertical displacement has almost the same order as the lateral one. The vertical vibrations also produce significant vertical inertia loads and shall be taken into account in design checks.

Aerodynamic admittance noticeably reduces the structural response by 26 % for vertical response and 40 % for rotating angle. Hereby, are used Sears functions, but they can underestimate admittance effect on response. Therefore, wind tunnel and CFD study shall be performed for extreme long bridges.

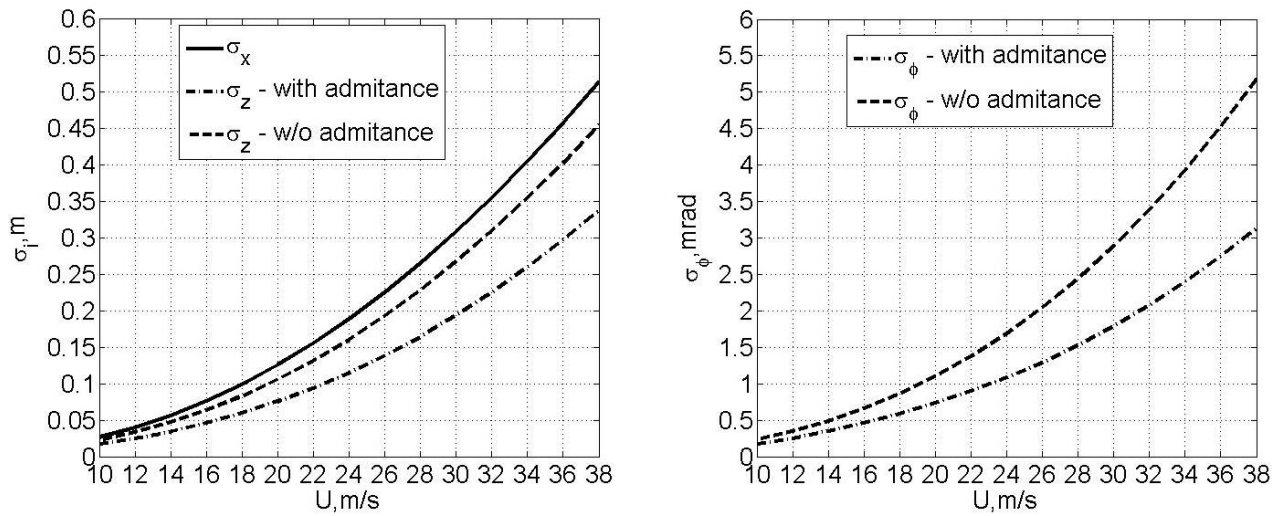


Figure 9. Standard deviation of lateral – u , vertical – w displacements and torsional ϕ rotation at the mid span.

Actually, the bridge buffeting response depends on type of bridge structural system, length of the main span, bridge deck aerodynamic properties and climate conditions.

The measured on site standard deviation for Lysefjord suspension bridge with 446 m main span are 0.1 m for lateral motion and 0.05 m at the middle of span for mean wind velocity 17.7 m/s [16]. The measured displacements are slightly less than analytical one. The response standard deviation derived from direct measuring in terms of acceleration for Norway Hardanger suspension bridge with span 1336 m is given in [17]. The most suitable values for comparison is data published in for Stonecutters bridge with main span 1018 m [13, 14]. The peak lateral buffeting response is 0.75 m and peak vertical response is 1.4 m for ocean exposure with wind velocity 52 m/s at the deck level. If we take peak factor equal to 3.5 we get standard deviation 0.21 m and 0.4 m for lateral and vertical response respectively. The Stonecutter bridge deck is 1.8 times wider than in the example. That is why the lateral response of Stonecutter bridge less than in the example.

Table 3 shows the results for the middle of the central span for design wind velocity 38 m/s at the 10 m height. After integrating Equation (17) according to Equation (22) we obtain the response variance. The variance has contribution of different parts of the structure and depends on correlation of turbulence components. The Table 3 explains the results as the ratio of each term in Equation (17) to the total response variance.

Table 3. Contribution of different structural elements and correlation of turbulence components into total response.

Response	Deck			Pylons u, u	Cables u, u
	u, u	w, w	u, w		
Lateral	0.391	0.161	0.151	0.084	0.295
Vertical	0.039	0.870	0.090	–	–
Torsional	0.101	1.073	–0.174	–	–

The main lateral response for long span bridges is the result of the deck and cable interaction with wind. It should be emphasized that the cables and the deck makes almost the same contribution into this response. Therefore, reducing the cable diameter and resistance to air flow is the main problem to be solved by the designer. Also noticeable contribution to the lateral response is given by the cross spectrum. The product sign of the drag coefficient and its slope is negative and the sign of the cross spectrum is also negative as it was mentioned above. This fact increases total lateral response. On the contrary, the torsional response is reduced due to the positive product of the pitch coefficient and its slope while covariance between longitudinal and vertical turbulence components is negative. If we compare the total response neglecting the cross spectrum with the total response, we find the lateral response increased by 8 % and the torsional response decreased by 8 %. However, vertical and torsional responses are marginally caused by derivatives of the steady state

aerodynamic coefficients. Thus, the deck shape options shall be considered carefully in terms of the steady state coefficients and their slopes. Besides, the steady state coefficients help the designer to assess the aerodynamic stability.

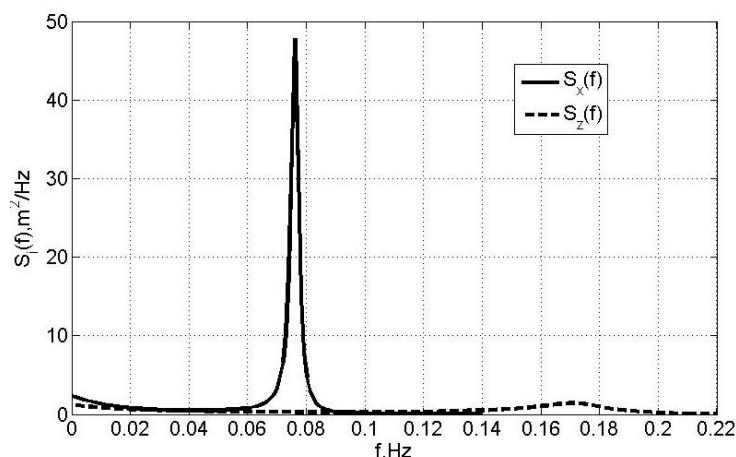


Figure 10. Power spectral density of the lateral – x , vertical – z displacements at the mid span.

The Van der Hoven spectra is represented by synoptic and turbulent parts. The synoptic part is considered as static wind load. The turbulent part is considered as dynamic wind action with peak around 0.02 Hz. The dynamic part with turbulent peak is described by power spectral density. According to Davenport the structural response can be represented as a sum of background and resonance components. The natural frequencies of the real bridges are quite separated from the turbulent spectral peak. The frequencies around 0.02 Hz contribute mostly to the background part of the total response. For the given example, (Figure 10) background part is 4 % of total dynamic response for lateral motion and include wind action within peak spectral frequency range.

On the Figure 10 is shown the power spectral density function of the lateral and vertical response. The response is divided into background response within range up to 0.02 Hz and the resonance response near the natural frequency. The lateral response has sharp resonance peak while the vertical one is shallow and wide due to significantly higher aerodynamic damping.

The general procedure for power law and logarithmic law is the same and using one of them depends on local climate condition and design code. The difference for both laws for the open terrain is very small. For the given example the difference in turbulent dynamic response is 7 % and 9 % in mean static response.

The real bridge structures within synoptic region about 0.02 Hz are hardly possible. For the given example, with lateral frequency 0.076 Hz the ratio of total response to the peak buffeting response is 1.89 for mid span.

4. Conclusion

1. The three component of wind velocity fluctuation as well as three aerodynamics forces shall be considered for long span cable stay analysis of structural response to turbulence wind flow.
2. The turbulence wind models for practical use in the absence of detailed site measurement proposed.
3. Analysis of structural response is based on the random stationary vibration theory under the assumption of small fluctuation velocities using steady state aerodynamic coefficients.
4. The simplified method of analysis using three main lateral, vertical and torsional modes is proposed. The method of cable system coherence analysis is presented.
5. The cable stay bridge with the main span of 1100 m is considered with the design wind velocity at the height of 10 m is considered. The power spectral density and the standard deviation response versus the wind velocity is obtained.
6. For the bridge deck shape in question the cross spectrum of the vertical component increases lateral response and reduce torsional one. The lateral response is caused mainly by the deck and cables. The deck and cables have almost equal contribution in the total response for the extremely long bridges.
7. The steady state coefficients shall be carefully considered when choosing the deck shape options.

8. The proposed method can be used for any dynamic excitation, which can be represented, by spectral densities and coherence and correlation functions. The linear resonance response can be analyzed by the methods of structural dynamic if excitation force is deterministic and known before calculation.

References

1. ESDU 85020. Characteristics of Atmospheric Turbulence Near the Ground – 2. Single Point Data for Strong Winds (Neutral Atmosphere). 2001.
2. ESDU 86010. Characteristics of Atmospheric Turbulence Near the Ground – 3. Variations in Space and Time for Strong Winds (Neutral Atmosphere). ESDU Data Items. 2001.
3. Simiu, E., Scanlan, R.H. Wind effects on structures : an introduction to wind engineering. New York, 1986.
4. EN 1991-1-4. Eurocode 1: Actions on structures – Part 1–4: General actions -Wind actions. European Committee for Standardization. 2005. DOI: ICS 91.010.30; 93.040.
5. Popov, N.A. Tornadoes and severe storms in Russia. Proceedings of the Conference on Natural Disaster Reduction. ASCE. Washington, D.C., 1996. Pp. 301–307.
6. Koljushev, I., Guzeev, R., Maslov, D. Engineering solutions for Golden Horn Bay bridge with V-shaped pylons. Long Span Bridges and Roofs – Development, Design and Implementation: 36th IABSE symposiumKolkata, 2013. Pp. 188–189.
7. Larsen, A. Advances in aeroelastic analyses of suspension and cable-stayed bridges. Journal of Wind Engineering and Industrial Aerodynamics. 1998. DOI: 10.1016/S0167-6105(98)00007-5.
8. Hui, M.C.H., Larsen, A., Xiang, H.F. Wind turbulence characteristics study at the Stonecutters Bridge site: Part I—Mean wind and turbulence intensities. Journal of Wind Engineering and Industrial Aerodynamics. 2009. 97(1). Pp. 22–36. DOI: 10.1016/J.JWEIA.2008.11.002.
9. Hui, M.C.H., Larsen, A., Xiang, H.F. Wind turbulence characteristics study at the Stonecutters Bridge site: Part II: Wind power spectra, integral length scales and coherences. Journal of Wind Engineering and Industrial Aerodynamics. 2009. 97(1). Pp. 48–59. DOI: 10.1016/J.JWEIA.2008.11.003.
10. Zhu, J., Zhang, W. Numerical simulation of wind and wave fields for coastal slender bridges. Journal of Bridge Engineering. 2017. 22(3). Pp. 1–17. DOI: 10.1061/(ASCE)BE.1943-5592.0001002.
11. Davenport, A.G. Buffeting of a suspension bridge by storm winds. Journal of the Structural Division. 1962. Vol. 88. Iss. 3. Pp. 233–270.
12. Jain, A., Jones, N.P., Scanlan, R.H. Coupled flutter and buffeting analysis of long-span bridges. Journal of Structural Engineering. 1996. 122(7). Pp. 716–725. DOI: 10.1061/(ASCE)0733-9445(1996)122:7(716).
13. Falbe-Hansen, K., Vejrum, T., Carter, M. Stonecutters Bridge – Design of the Steel Superstructure. Steelbridge 2004, Steel bridges extend structural limits. (June 2004)Millau, 2004. Pp. 1–18.
14. Hui, M.C.H., Ding, Q.S., Xu, Y.L. Buffeting Response Analysis of Stonecutters Bridge. HKIE Transactions. 2005. 12(2). Pp. 8–21. DOI: 10.1080/1023697X.2005.10667998.
15. Fenerci, A., Øiseth, O., Rønquist, A. Long-term monitoring of wind field characteristics and dynamic response of a long-span suspension bridge in complex terrain. Engineering Structures. 2017. DOI: 10.1016/j.engstruct.2017.05.070.
16. Cheynet, E., Jakobsen, J.B., Snæbjörnsson, J. Buffeting response of a suspension bridge in complex terrain. Engineering Structures. 2016. 128. Pp. 474–487. DOI: 10.1016/J.ENGSTRUCT.2016.09.060.
17. Fenerci A., Øiseth, O. Full-Scale Measurements on the Hardanger Bridge During Strong Winds. Dynamics of Civil Structures, Volume 2. Conference Proceedings of the Society for Experimental Mechanics Series. Springer. Cham, 2016.
18. Khrapunov, E.F., Solovov, S.Y. Modeling of the mean wind loads on structures. Magazine of Civil Engineering 2019. 88(4). Pp. 42–51. DOI: 10.18720/MCE.88.4.
19. Lingu, D., Gelder, P. Characteristics of Wind Turbulence With. 2nd European & African Conference on Wind Engineering. Vol. 2Genova, 1997. Pp. 1271–1277.
20. Solari, G., Piccardo, G. Probabilistic 3-D turbulence modeling for gust buffeting of structures. Probabilistic Engineering Mechanics. 2001. 16(1). Pp. 73–86. DOI: 10.1016/S0266-8920(00)00010-2.
21. Yan, L., Zhu, L.D., Flay, R.G.J. Span-wise correlation of wind-induced fluctuating forces on a motionless flat-box bridge deck. Journal of Wind Engineering and Industrial Aerodynamics. 2016. 156. Pp. 115–128. DOI: 10.1016/J.JWEIA.2016.07.004.
22. Katsuchi, B.H., Jones, N.P., Scanlan, R.H., Member, H. Multimode Coupled Flutter and Buffeting Analysis of the Akashi-Kaikyo Bridge. Journal of Structural Engineering. 1999. Pp. 60–70. DOI: 10.1061/(asce)0733-9445(1999)125:1(60).
23. Fung, Y.C. An Introduction to the Theory of Aeroelasticity. Dover. New York, 1969.
24. Horlock, J.H. Fluctuating Lift Forces on Aerofoils Moving Through Transverse and Chordwise Gusts. Journal of Basic Engineering. 1968. 90. Pp. 494–500. DOI: 10.1115/1.3605173.
25. Hejlesen, M.M., Rasmussen, J.T., Larsen, A., Walther, J.H. On estimating the aerodynamic admittance of bridge sections by a mesh-free vortex method. Journal of Wind Engineering and Industrial Aerodynamics. 2015. 146. Pp. 117–127. DOI: 10.1016/j.jweia.2015.08.003.
26. Zhao, L., Ge, Y. Cross-spectral recognition method of bridge deck aerodynamic admittance function. Earthquake Engineering and Engineering Vibration. 2015. 14(4). Pp. 595–609. DOI: 10.1007/s11803-015-0048-8.

Contacts:

Roman Guzeev, +78124980925; guzeev.roman@gmail.com

Andreas Domaingo, +4331626978636; adomaingo@allplan-infra.com



DOI: 10.18720/MCE.93.4

Реакция большепролетных мостов на турбулентный ветровой поток

Р.Н. Гузеев^а, А. Доминго^б

^а Санкт-Петербургский государственный архитектурно-строительный университет, Санкт-Петербург, Россия

^б ALLPLAN Infrastructure GmbH, Грац, Австрия

* E-mail: guzeev.roman@gmail.com

Ключевые слова: вантовые и висячие мосты, динамический отклик, модели турбулентности, пролетное строение моста, проектирование конструкций, когерентность, случайные колебания, численные модели.

Аннотация. Изучен отклик вантовых мостов на воздействие пульсационной ветровой нагрузки. Обобщены несколько моделей ветрового потока и предложены модели для практического применения. Модель ветрового потока включает в себя профили средней скорости и интенсивности турбулентности, энергетические спектры и функции пространственной когерентности. Динамический отклик конструкции определяется теорией случайных колебаний для стационарного случайного процесса. Предложен упрощенный метод расчета, используя разложение по собственным формам колебаний с учетом только основных форм. Аэродинамическое демпфирование вычисляется с использованием производных флаттера. Разработан метод учета пространственной когерентности ветровой нагрузки для вантовой системы. Предложена процедура вычисления обобщенной спектральной плотности пульсационной ветровой нагрузки для различных конструктивных элементов, которая учитывает влияние трех компонент пульсаций скорости ветра. Проанализирован вклад различных компонент пульсаций скорости ветра и их корреляция в полный динамический отклик различных элементов конструкции.

Литература

- ESDU 85020. Characteristics of Atmospheric Turbulence Near the Ground – 2. Single Point Data for Strong Winds (Neutral Atmosphere). 2001.
- ESDU 86010. Characteristics of Atmospheric Turbulence Near the Ground – 3. Variations in Space and Time for Strong Winds (Neutral Atmosphere). ESDU Data Items. 2001.
- Simiu E., Scanlan R.H. Wind effects on structures : an introduction to wind engineering. New York, 1986.
- EN 1991-1-4. Eurocode 1: Actions on structures – Part 1–4: General actions -Wind actions. European Committee for Standardization. 2005. DOI: ICS 91.010.30; 93.040.
- Popov N.A. Tornadoes and severe storms in Russia. Proceedings of the Conference on Natural Disaster Reduction. ASCE. Washington, D.C., 1996. Pp. 301–307.
- Koljushev I., Guzeev R., Maslov D. Engineering solutions for Golden Horn Bay bridge with V-shaped pylons // Long Span Bridges and Roofs – Development, Design and Implementation: 36th IABSE symposium Kolkata, 2013. Pp. 188–189.
- Larsen A. Advances in aeroelastic analyses of suspension and cable-stayed bridges // Journal of Wind Engineering and Industrial Aerodynamics. 1998. DOI: 10.1016/S0167-6105(98)00007-5.
- Hui M.C.H., Larsen A., Xiang H.F. Wind turbulence characteristics study at the Stonecutters Bridge site: Part I—Mean wind and turbulence intensities // Journal of Wind Engineering and Industrial Aerodynamics. 2009. 97(1). Pp. 22–36. DOI: 10.1016/J.JWEIA.2008.11.002.
- Hui M.C.H., Larsen A., Xiang H.F. Wind turbulence characteristics study at the Stonecutters Bridge site: Part II: Wind power spectra, integral length scales and coherences // Journal of Wind Engineering and Industrial Aerodynamics. 2009. 97(1). Pp. 48–59. DOI: 10.1016/J.JWEIA.2008.11.003.
- Zhu J., Zhang W. Numerical simulation of wind and wave fields for coastal slender bridges // Journal of Bridge Engineering. 2017. 22(3). Pp. 1–17. DOI: 10.1061/(ASCE)BE.1943-5592.0001002.
- Davenport A.G. Buffeting of a suspension bridge by storm winds // Journal of the Structural Division. 1962. Vol. 88(Issue 3). Pp. 233–270.
- Jain A., Jones N.P., Scanlan R.H. Coupled flutter and buffeting analysis of long-span bridges // Journal of Structural Engineering. 1996. 122(7). Pp. 716–725. DOI: 10.1061/(ASCE)0733-9445(1996)122:7(716).
- Falbe-Hansen K., Vejrum T., Carter M. Stonecutters Bridge – Design of the Steel Superstructure // Steelbridge 2004, Steel bridges extend structural limits. (June 2004) Millau, 2004. Pp. 1–18.
- Hui M.C.H., Ding Q.S., Xu Y.L. Buffeting Response Analysis of Stonecutters Bridge // HKIE Transactions. 2005. 12(2). Pp. 8–21. DOI: 10.1080/1023697X.2005.10667998.

15. Fenerci A., Øiseth O., Rønquist A. Long-term monitoring of wind field characteristics and dynamic response of a long-span suspension bridge in complex terrain // *Engineering Structures*. 2017. DOI: 10.1016/j.engstruct.2017.05.070.
16. Cheynet E., Jakobsen J.B., Snæbjörnsson J. Buffeting response of a suspension bridge in complex terrain // *Engineering Structures*. 2016. 128. Pp. 474–487. DOI: 10.1016/J.ENGSTRUCT.2016.09.060.
17. Fenerci A., Øiseth O. Full-Scale Measurements on the Hardanger Bridge During Strong Winds // *Dynamics of Civil Structures*. Vol. 2. Conference Proceedings of the Society for Experimental Mechanics Series. Springer. Cham, 2016.
18. Соловьев С.Ю., Храпунов Е.Ф. Моделирование средних ветровых нагрузок на сооружения // *Инженерно-строительный журнал*. 2019. № 4(88). С. 42–51. DOI: 10.18720/MCE.88.4
19. Lingu D., Gelder P. Characteristics of Wind Turbulence With // *2nd European & African Conference on Wind Engineering*. Vol. 2Genova, 1997. Pp. 1271–1277.
20. Solari G., Piccardo G. Probabilistic 3-D turbulence modeling for gust buffeting of structures // *Probabilistic Engineering Mechanics*. 2001. 16(1). Pp. 73–86. DOI: 10.1016/S0266-8920(00)00010-2.
21. Yan L., Zhu L.D., Flay R.G.J. Span-wise correlation of wind-induced fluctuating forces on a motionless flat-box bridge deck // *Journal of Wind Engineering and Industrial Aerodynamics*. 2016. 156. Pp. 115–128. DOI: 10.1016/J.JWEIA.2016.07.004.
22. Katsuchi B.H., Jones N.P., Scanlan R.H., Member H. Multimode Coupled Flutter and Buffeting Analysis of the Akashi-Kaikyo Bridge // *Journal of Structural Engineering*. 1999. Pp. 60–70. DOI: 10.1061/(asce)0733-9445(1999)125:1(60).
23. Fung Y.C. An Introduction to the Theory of Aeroelasticity. Dover. New York, 1969.
24. Horlock J.H. Fluctuating Lift Forces on Aerofoils Moving Through Transverse and Chordwise Gusts // *Journal of Basic Engineering*. 1968. 90. Pp. 494–500. DOI: 10.1115/1.3605173.
25. Hejlesen M.M., Rasmussen J.T., Larsen A., Walther J.H. On estimating the aerodynamic admittance of bridge sections by a mesh-free vortex method // *Journal of Wind Engineering and Industrial Aerodynamics*. 2015. 146. Pp. 117–127. DOI: 10.1016/j.jweia.2015.08.003.
26. Zhao L., Ge Y. Cross-spectral recognition method of bridge deck aerodynamic admittance function // *Earthquake Engineering and Engineering Vibration*. 2015. 14(4). Pp. 595–609. DOI: 10.1007/s11803-015-0048-8.

Контактные данные:

Роман Николаевич Гузеев, +78124980925; эл. почта: guzeev.roman@gmail.com

Андреас Доминго, +4331626978636; эл. почта: adomaingo@allplan-infra.com